Influence of steel cleanliness on drawability of fine filaments with high tensile strength

Julie Godon, Pascal Antoine, Jean-Bernard Vogt, Jeremie Bouquerel

Metall. Res. Technol. **116**, 513 (2019)

https://doi.org/10.1051/metal/2019025

Inclusion cleanliness in the metallic alloys
Edited by Jean-Pierre Bellot, Pascal Gardin, Frédéric Gruy

Metallurgical Research & Technology

Available online at:
www.metallurgical-research.org

Regular Article

Open Access

Influence of steel cleanliness on drawability of fine filaments with high tensile strength

Julie Godon[1,2], Pascal Antoine[2], Jean Bernard Vogt[1,*], and Jérémie Bouquerel[1]

[1] Univ. Lille, CNRS, INRA, ENSCL, UMR 8207 – UMET – Unité Matériaux et Transformations, 59000 Lille, France
[2] Bekaert NV, Bekaertstraat 2, 8550 Zwevegem, Belgique

Received: 21 December 2018 / Accepted: 26 April 2019

Abstract. The aim of the current study is to clarify the influence of steel cleanliness on the fracture during wet wire drawing of high strength high carbon very fine filaments. Methodologies for inclusion identification and for inclusion count were developed. Ninety percent of the fractured filaments were associated with an inclusion which was SiO_2, or SiO_2-CaO or SiO_2-MgO. The fracture of the wires resulted from debonding of the inclusion from the matrix. Inclusion density assessed from total oxygen content in the wire was successfully and reliably obtained. Inclusions exhibited a wide range of sizes but mostly around 6 μm. The inclusion density did not appear as the only parameter that affects the fracture occurrence. An important effect of size and of chemical composition of the inclusions was found. A critical size of inclusions for fracture was observed but it depends on the chemical composition of inclusions.

Keywords: inclusions / steel cleanliness / wire drawing / fracture / steel filament

1 Introduction

Non-metallic inclusions play an important role on crack initiation and further fracture of metallic alloys subjected to mechanical loading. This can occur during service of the material as well as during processing. Respectively, fracture associated with non-metallic inclusions has been observed when the material is under fatigue [1–3] or when it is wiredrawn or rolled [4]. Though these two situations strongly differ in the loading level, it is shown that the presence of a single inclusion can be detrimental enough to lead to fracture. Attention is today much paid on the role of inclusions on fatigue resistance especially in very high cycle fatigue. Unfortunately, it is very hazardous to transfer directly the acquired knowledge in the field of fatigue to the field of wire drawing or cold rolling. Indeed, these processes involve huge amount of monotonic plastic deformation which can result to very thin sheet or very small diameter of wire.

For some applications (filters, saw wires, wire ropes...), superfine steel wires are needed. The market requires very fine wires with very high mechanical properties. However, fractures might occur during the wet wire drawing process that leads to 60 μm filaments. The main types of fracture during drawing fine filaments are central bursting, tension break and fracture due to inclusions. The main feature of fine filaments is that the size of the inclusion approaches the diameter of the wire so that only one single inclusion can be responsible for the fracture. Very fine wires are currently processed on tungsten [5], gold [6] and copper [7–9]. Both process parameters (drawing speed, die angle...) and inclusions properties (shape, size...) were found to influence the drawability. Steel wires are more complicated to be studied because of the complexity of the microstructure being generally multiphased. Some studies shows the impact of inclusions on steel wire for bigger diameter by finite element analysis (FEA) [10,11]. Nevertheless, the identification of inclusion characteristics is a prerequisite for the understanding of failure mechanism of very fine wires. The characterization of inclusions includes chemical, mechanical and morphological aspect [12,13]. The quality of the results depends on the number of analyzed inclusions which extraction is easier in bulk material than in fine wires.

The present paper deals with the fracture of very fine wires of pearlitic steels with diameter less than 80 μm. It aims first at pointing out the importance of the presence of inclusions. Then it focuses on the determination of the inclusions characteristics (size, chemical composition, shape) and on their impact on fracture occurrence during the fine filament drawing.

* e-mail: jean-bernard.vogt@univ-lille.fr

Table 1. Chemical composition of wire rods (wt.%).

C	Mn	Si	Cr	Ni	S	P	Fe
0.94−1.02	0.3	0.2	0.2	0.01	< 0.01	< 0.01	Bal.

2 Materials and methods

2.1 Materials

The investigated filaments have been drawn from wire rods of 5.5 mm in diameter provided by different suppliers. The typical chemical composition is reported in Table 1, the carbon content of the wires varies from 0.94 to 1.02%C. It is assumed that carbon content only influences mechanical properties but not the inclusion composition and their density.

The cleanliness quality of the steel was dependent upon the steelmaker. It is defined by the density and the composition of non-metallic inclusions present in the wire.

Rods of 5.5 mm were transformed by several steps of dry wire drawing and heat treatment. During the final step called wet wire drawing (WWD), the intermediate wire was drawn into filaments of diameter down to 60 µm by more than 20 passes.

2.2 Experimental procedure

For assessment of the inclusion morphology, the Dekker extraction method [14] was employed in order to dissolve the matrix and to recover the inclusions. The chemical solution contained a mixture of HNO_3, H_2SO_4 and H_2O in the respective proportion 1%:38%:61%.

All filaments that fractured during WWD were collected for fracture surface observations and chemical analysis of the inclusions by scanning electron microscopy (SEM). This was performed on a FEI Quanta 200 3D SEM coupled with the Oxford Instruments EDS system and operating at an accelerating voltage of 15 kV.

The size of the encountered inclusions was determined by means of equivalent circular diameter (ECD) as defined by equation (1). For calculation hypothesis, the inclusions were considered with an ovoid shape:

$$\mathrm{ECD} = (4 * S_{\mathrm{inc}}/\pi)^{0.5}, \tag{1}$$

where S_{inc} is the surface inclusion defined by equation (2):

$$S_{\mathrm{inc}} = r_L * r_w * \pi. \tag{2}$$

Here, r_L is the radius of the length of the inclusion and r_w the radius of the width of the inclusion.

To define the morphology of inclusions, the aspect ratio of the inclusions is defined as follows:

$$\text{Aspect ratio} = r_L/r_w.$$

An aspect ratio of 1 corresponds to a spherical inclusion and higher is the value, the more elongated is the inclusion.

For the investigation of the cleanliness of the steel, automated SEM/EDS analysis of polished longitudinal section specimen were performed using a JEOL 7200F FEG-SEM and an Oxford Instruments EDS system. The automated inclusions measurement with SEM/EDS provided the size of inclusions, the number of inclusions, and the chemical composition of the inclusions. Inclusion density was calculated as follows (Eq. (3)):

$$d_{\mathrm{inc}} = \frac{n}{S_{\mathrm{total}}}, \tag{3}$$

where d_{inc} is the density of inclusions per/cm^2, n is the number of detected inclusions, S_{total} is the total scanned area.

In addition to the SEM/EDS technique, the cleanliness was also evaluated by oxygen measurement using a combustion technique with a LECO TC500. Indeed, the total oxygen content can be a reasonable indirect way to evaluate the total amount of oxide inclusions in steel [13].

3 Results and discussion

3.1 Fracture cause

More than 200 fractured filaments during WWD were investigated in order to determine the fracture cause. Fracture surfaces of filaments either contained an inclusion (Fig. 1a) or were free of inclusion (Fig. 1b).

An inclusion was present in more than 90% of the fractures. Although this ratio appears much higher than that reported in the literature [7] for copper (52%), it is closer to the one observed for inclusion related fracture on bigger diameter steel wire (80%) [10]. Inclusions into fracture surface are always in the centre of the wire and on the top of a cone fracture.

When an inclusion was not involved in the fracture of the filament, the latter exhibited a slight necking and the fracture surface contained dimples. Therefore, though the filament was strongly deformed during the drawing process, it kept a certain degree of ductility.

3.2 Identification of inclusions

3.2.1 Chemical composition

EDS analysis were performed directly on the inclusions emerged from the fracture surfaces (Figs. 2a–2c). Three major types of inclusions were identified on the fracture surfaces.

All the analysed inclusions have been identified as Si-based inclusions. The latter were pure silicon oxide (SiO_2) (Fig. 2a) or a more complex composition SiO_2-CaO (Fig. 2b) or SiO_2-MgO (Fig. 2c). CaO and MgO refer to the second major compound present into the inclusion.

Si-type inclusions appear to be non-deformable during wire drawing of fine filaments [15].

Figure 2 shows also the different morphologies of inclusion responsible for fracture. The SiO_2 inclusions appeared to be rather round while SiO_2-MgO appeared to be rectangular with sharp angles. The shape of SiO_2-CaO inclusions was difficult to appreciate by this technique.

In order to evaluate the inclusions morphology as well as their effect on the surrounding matrix, sectional analysis of the fractures was carried out (Figs. 3a and 3b). For both cone and cup part of the fracture, it appears that some

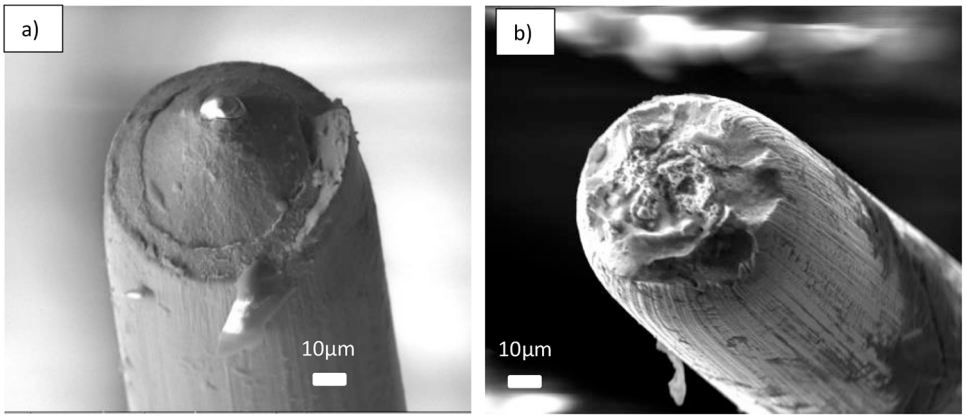

Fig. 1. Fracture surfaces of filaments a) containing an inclusion, b) free of inclusion.

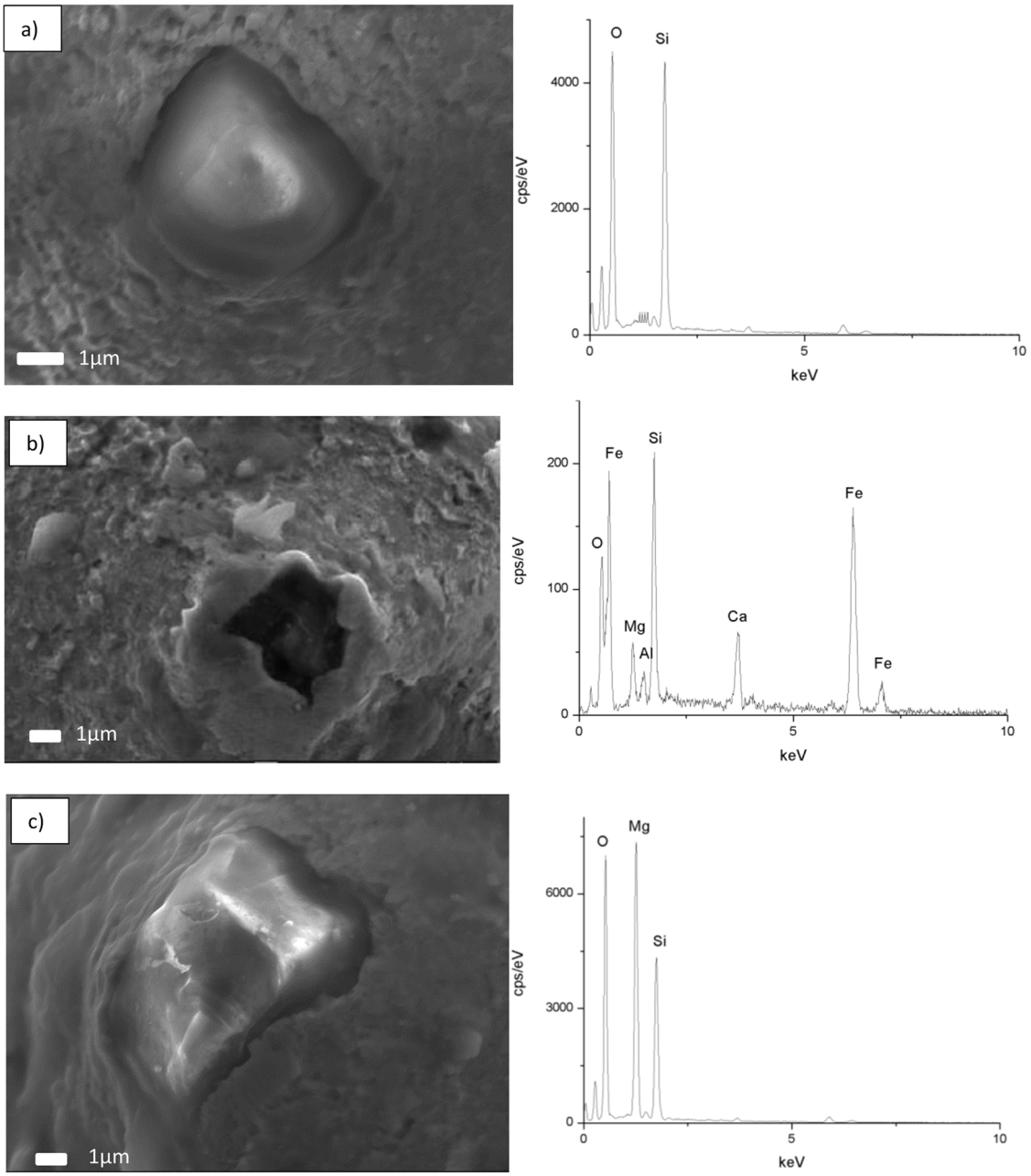

Fig. 2. SEM images and EDS spectra of typical inclusions found on fracture surfaces. a) SiO_2; b) SiO_2-CaO; c) SiO_2-MgO.

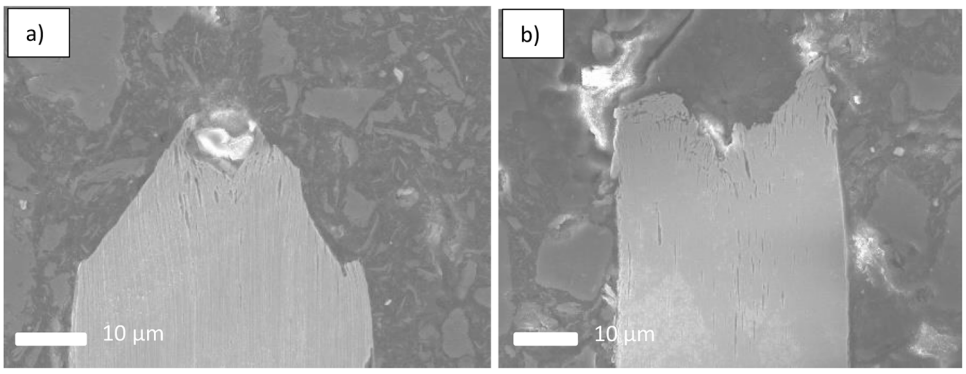

Fig. 3. Longitudinal section of fractured wires obtained during WWD. a) SE image of cone part of the fracture; b) SE image of the cup part of the fracture.

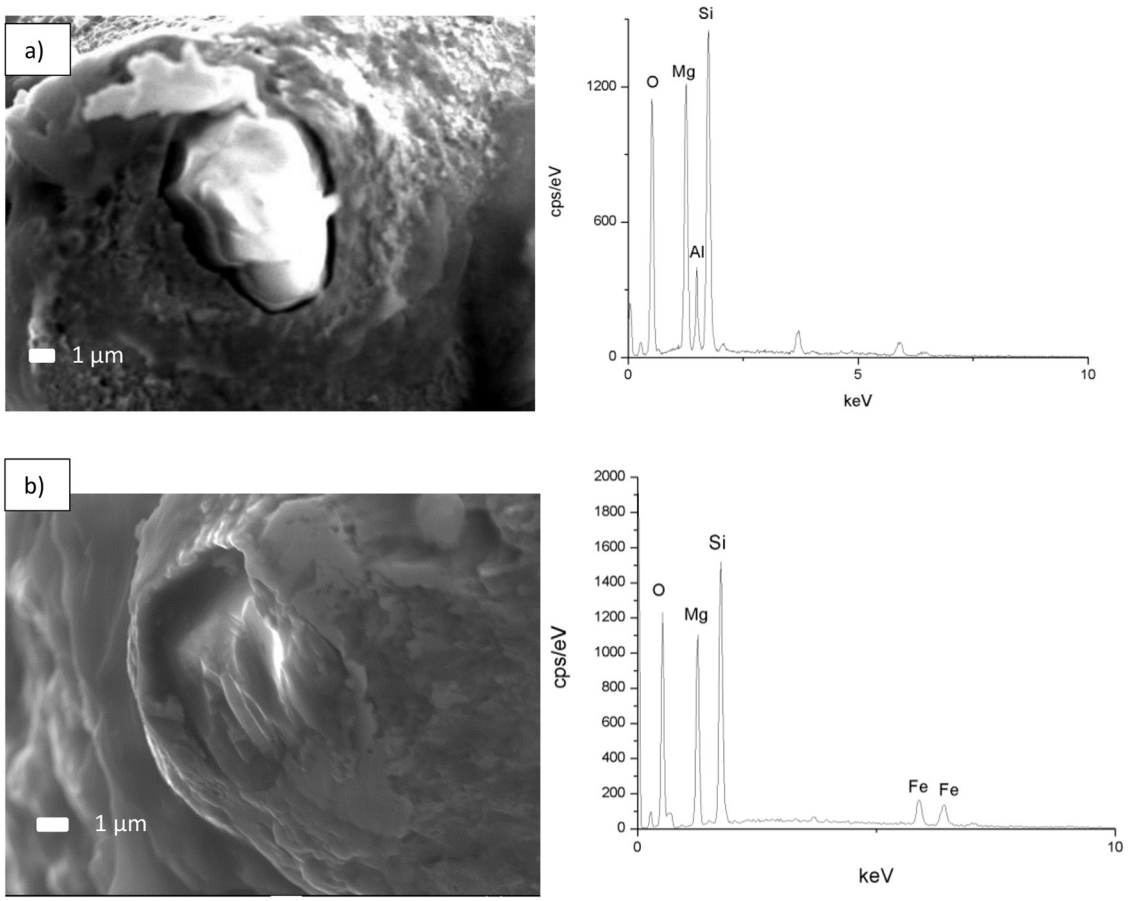

Fig. 4. Effect of chemical composition of inclusion on sensitivity to debonding. a) Rich-Al inclusion; b) Al-free inclusion.

defects parallel to the drawing axis are present around the inclusion, however no real crack opening are observed along the drawing axis.

Some inclusions seem to be more prone for debonding. The presence of certain chemical elements is known to play a role on debonding of the inclusion into the fracture. Here, this aspect is confirmed as shown in Figure 4. Hence, the aluminium-rich inclusion (Fig. 4a) appears more prone to debonding than the alumium-free one (Fig. 4b). This statement is in correlation with the study of where the aluminium content is proved to be promoting the debonding matrix/inclusion during fatigue test [16].

3.2.2 Size

The identified inclusions also differed in their ECD as well as in their quantity as shown in Figure 5. The size of inclu sions involved in filament fracture is ranging from 1.90 to 23 µm but the majority of inclusions exhibits an average of ECD of 6 ± 3 µm.

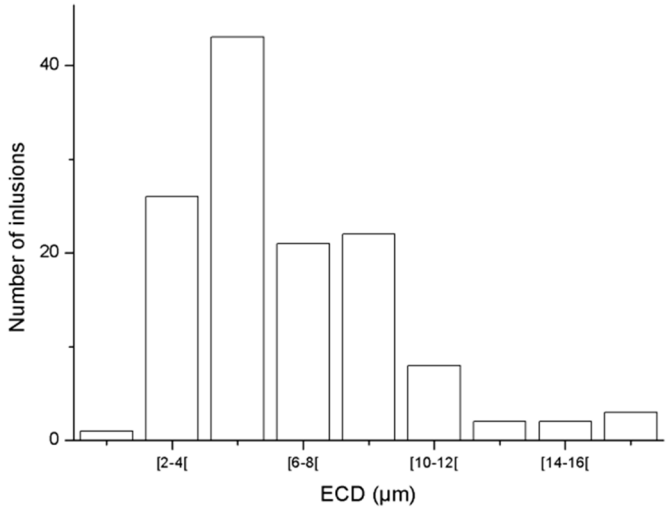

Fig. 5. ECD distribution of the critical inclusions present into fracture surfaces.

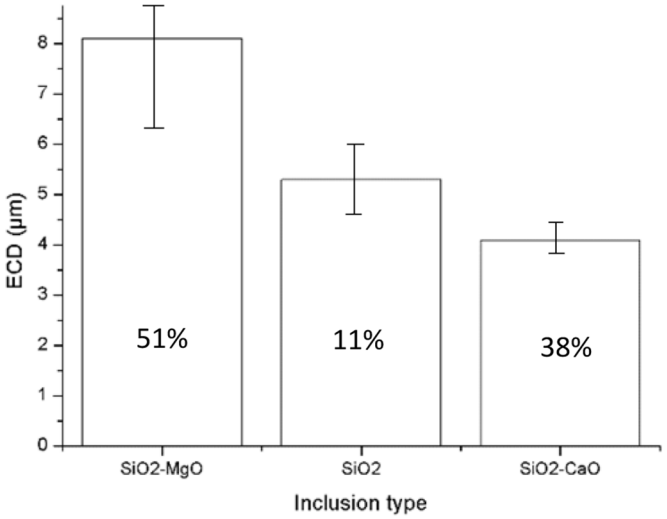

Fig. 6. Critical size of inclusions causing fracture.

A link between the composition and the critical size of inclusions found on fracture surfaces is observed. The chemical composition is expected to influence the critical size of the inclusion for drawability by different ways. By means of FEA, Yu et *al.* [17] pointed out cracks near inclusions after rolling as a result of a non-uniform deformation around the inclusion which was emphasized with increasing the inclusion size. As well, the inclusion size and inclusion composition impact the fatigue properties by changing the local stress state in and around the non-metallic inclusions as a result of the strong difference in Young modulus between the inclusion and the matrix [11].

Although Si-inclusions are known to be non-deformable during forming process [15], secondary major elements also exhibit an effect in regards to the WWD process. Hence, the critical size of the inclusions involved in the fracture is dependent of the CaO and MgO presence. Indeed, CaO decreases the critical size of the inclusions leading to fracture, whereas MgO tends to increase it.

Figure 6 shows the amount of fractures related to each type of inclusions. SiO_2-MgO inclusions are the most frequently encountered (51%) while SiO_2 inclusions seem to be less dangerous for fracture occurrence (11%). Furthermore, variations in hardness between these inclusions are expected.

However, even if the SiO_2-CaO inclusions are responsible of 38% of the fractures, a statistical analysis of the distribution of the inclusions within the wire rod (Tab. 2) indicates that this type of inclusions is only present on 17% of all the inclusions present into the wire.

Table 2. Proportion of each inclusion type measured by automated SEM/EDS on wire rod.

Inclusion type	SiO_2	SiO_2-MgO	SiO_2-CaO
Proportion (%)	31	52	17

3.4 Factors promoting fracture

3.4.1 Inclusion density

The first parameter suspected to have an influence on fracture occurrence was the inclusion density. Indeed, as it is claimed that the cleanliness of steel wire has an impact on the drawability of wires, the relationship between inclusion density and fracture is one of the points to consider. Here, the drawability has been evaluated by counting the number of fractures encountered per 1 ton of processed material. When the number of fracture per ton exceed a predefined threshold $(Th_{inc-1\,ton})^*$, the material was considered bad in term of drawability. Otherwise, the material is considered good for processing. In order to pre scan the inclusion population, the cleanliness was assessed from LECO oxygen measurement. The LECO device measures the total oxygen contained in the steel while SEM/EDS provides a density of inclusions containing oxygen. Figure 7a shows that there is a simple relation between the total oxygen content (O_{tot}) and the oxide density. Hence, a reliable link between the oxide density and the measurement of the total oxygen content O_{tot} relation can be established.

Comparing drawability and oxide density (Fig. 7b) points out a general tendency. An exceptional drawability is observed for very low oxide density (about 50 inclusions per cm^2). For higher oxide densities, the scattering does not allow establishing a clear correlation. The wires classified as bad in terms of drawability contained an oxide density below 400 inclusions per cm^2. However, even with this density or higher (up to 600 inclusions per cm^2), some wires had satisfied the qualification. Therefore, the oxide density estimated by the measurement of total oxygen content provides a first idea of the global drawability. It is encouraged to decrease the oxide density in the steel for decreasing the amount of fracture per ton during the WWD. However, one must have in mind that there is no clear oxide density threshold below which will result in a good or bad drawability. In conclusion, the oxide density is not the only factor that has an influence on the number of

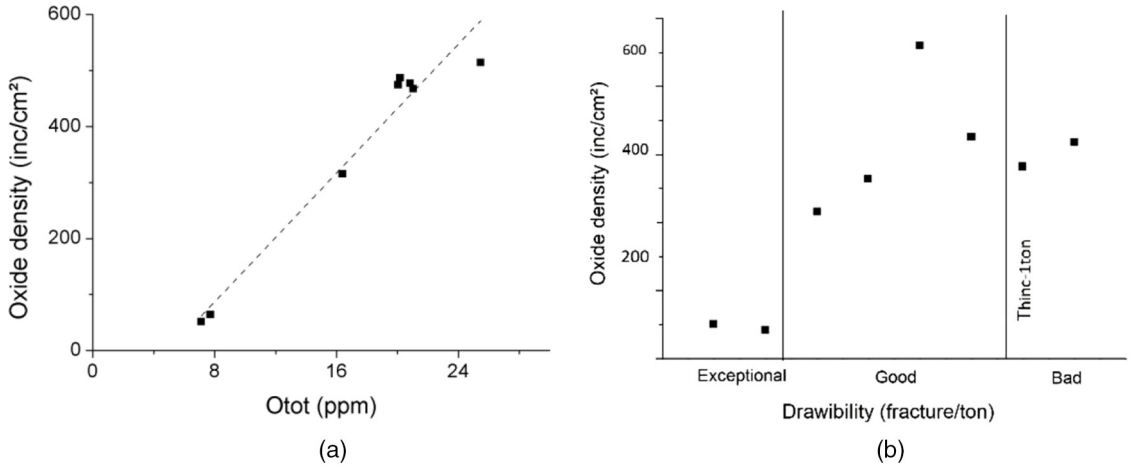

Fig. 7. a) Relation between O_{tot} and oxide density; b) Effect of oxide density on drawability.

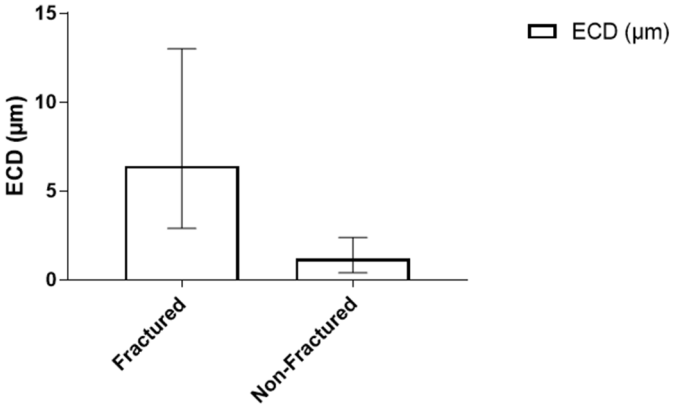

Fig. 8. Effect of the inclusion size on fracture occurrence of wires.

fractures per ton. The drawability depends also on inclusions properties such as the size, the morphology and the chemical composition.

3.4.2 Inclusion size effect

Both fractured and non-fractured filaments have been investigated in order to consider if one of the inclusion features appeared to be the most relevant for the fracture. Fine filaments were embedded and polished so that the longitudinal section could be observed. One hundred inclusions in a non-fractured filament were examined by SEM. It was found that there was no preferential inclusion in terms of chemical composition in the fractured and non-fractured wires. All the types of morphologies were found in fractured and non-fractured filaments.

However, it has been found that the average size of inclusions in the non-fractured wires is much lower than that in the fractured filaments (Fig. 8). Indeed, it turns out that there is a critical size of about 3 µm for the inclusion to cause the fracture of the filament. Independently of the chemical composition, inclusions lower than 3 µm are considered as not dangerous for WWD of 60 µm filaments. This implies that not only the quantity on inclusions present into the wire is important but also the size of the inclusions.

3.4.3 Effect of inclusion shape

Beside the chemical characterisation of the inclusions, their morphologies have also been assessed.

The precipitates retrieved from the dissolved matrix were observed by SEM to obtain the 3D morphology together with the composition. SiO_2 inclusions have a rounded shape with an aspect ratio equal in average to 1.05 which translates a spherical shape. (Fig. 9a), SiO_2-CaO inclusions (Fig. 9b) present an ovoid shape and an aspect ratio average of 1.26. While SiO_2-MgO inclusions are mainly rectangular with sharp angle and elongated with an aspect ratio of 1.37 (Fig. 9c). The identification of the inclusions with the extraction method confirms and defines the morphology of inclusions assessed on fractures. SiO_2-MgO particles exhibit sharp angles, suggesting therefore they could act as stress concentrators [18] and accelerate the process of fracture. However, this was not just the case.

4 Conclusion

The present study aims at linking the fracture of very fine filaments of pearlitic steels with the presence of inclusions and leads to the following conclusions:

- inclusions are responsible of fractures for more than 90% of the case during WWD;
- three main types of inclusions have been found: SiO_2, SiO_2-CaO and SiO_2-MgO;
- the fracture of the wires results from the debonding of the inclusion from the matrix;
- the inclusion density does not control alone the drawability but also the composition, size and morphology of inclusions;
- the chemical composition of inclusions plays a role on the critical size of inclusions for fracture.

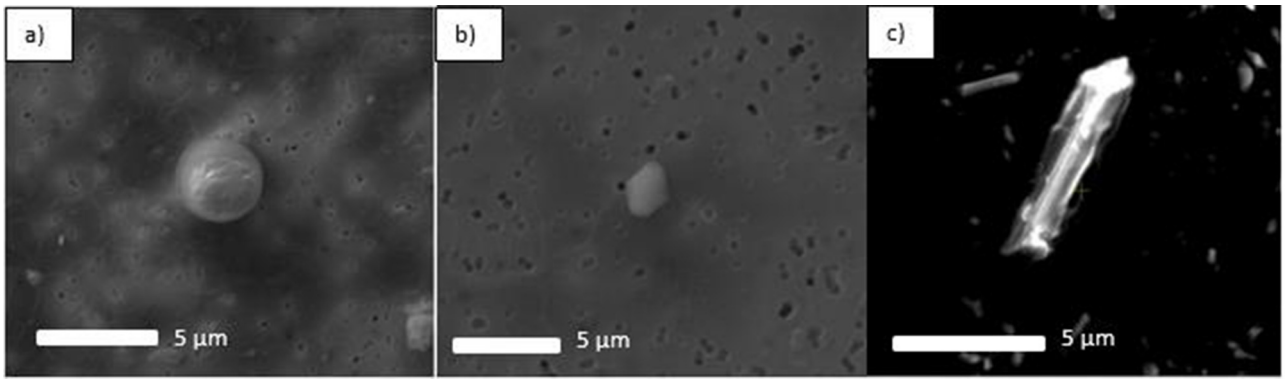

Fig. 9. Different inclusion morphology after dissolution. a) SiO_2; b) SiO_2-CaO; c) SiO_2-MgO.

Nomenclature

SEM	Scanning electron microscope
EDS	Energy-dispersive X-ray spectroscopy
WWD	Wet wire drawing
ECD	Equivalent circular diameter
FEA	Finite element analysis
O_{tot}	Oxygen total measured of the wire
S_{inc}	Surface of the inclusion
d_{inc}	Inclusion density (inc/cm^2)
r_l	Radius of the length of the inclusion (µm)
r_w	Radius of the width of the inclusion (µm)

References

1. D. Spriestersbach, P. Grad, E. Kerscher, Influence of different non-metallic inclusion types on the crack initiation in high-strength steels in the VHCF regime, Int. J. Fatigue **64**, 114–120 (2014)
2. C. Ruffing, Y. Ivanisenko, E. Kerscher, A comparison of the fatigue and fracture behavior of high strength ultrafine grained medium carbon steel SAE 1045 with high strength bearing steel SAE 52100, Procedia Struct. Integr. **2**, 3240–3247 (2016). doi: 10.1016/j.prostr.2016.06.404
3. K. Lambrighs, I. Verpoest, B. Verlinden, M. Wevers, Influence of non-metallic inclusions on the fatigue properties of heavily cold drawn steel wires, Procedia Eng. **2**, 173–181 (2010)
4. W. Yan, H.C. Xu, W.Q. Chen, Study on inclusions in wire rod of tire cord steel by means of electrolysis of wire rod, Steel Res. Int. **85**, 53–59 (2014)
5. P. Schade, Wire drawing failures and tungsten fracture phenomena, Int. J. Refract. Met. Hard Mater. **24**, 332–337 (2006)
6. S.B. Son, Y.K. Lee, S.H. Kang, H.S. Chung, J.S. Cho, J.T. Moon, K.H. Oh, A numerical approach on the inclusion effects in ultrafine gold wire drawing process, Eng. Fail. Anal. **18**, 1272–1278 (2011)
7. S. Norasethasopon, K. Yoshida, Finite element analysis on drawing of copper wire containing an inclusion and a cavity, Kejuruteraan **15**, 83–95 (2003)
8. S. Norasethasopon, K. Yoshida, Influence of an inclusion on multi-pass copper shaped-wire drawing by 2D finite element analysis, IJE Trans. **16**, 279–292 (2003)
9. S. Norasethasopon, K. Yoshida, Influences of inclusion shape and size in drawing of copper shaped-wire, J. Mater. Process. Technol. **172**, 400–406 (2006)
10. M. Yilmaz, Failures during the production and usage of steel wires, J. Mater. Process. Technol. **171**, 232–239 (2006)
11. S.-I. Ji, K.-H. Lee, Y.-S. Yang, The effects of non-metallic inclusions on ductile damage of high carbon steel wire in multi-pass dry drawing process, Key Eng. Mater. **622–623**, 155–161 (2014)
12. L. Zhang, B.G. Thomas, X. Wang, K. Cai, Evaluation and control of steel cleanliness: Review, 85th Steelmak. Conf. ISS-AIME, Warrendale, PA, 2002, pp. 431–452
13. L.F. Zhang, B.G. Thomas, State of the art in evaluation and control of steel cleanliness, ISIJ Int. **43**, 271–291 (2003)
14. Rob Dekkers, Ph.D. Thesis, Katholieke Universiteit Leuven, Leuven, Belgium, 2002
15. S. Feichtinger, S. Michelic, Y. Kang, In situ observation of the dissolution of SiO_2 particles in CaO-Al_2O_3-SiO_2 slags and mathematical analysis of its dissolution pattern, J. Am. Ceram. Soc. **97**, 316–325 (2014)
16. Y. Hu, W. Chen, C. Wan, F. Wang, H. Han, Effect of deoxidation process on inclusion and fatigue performance of spring steel for automobile suspension, Metall. Mater. Trans. B **49(2)**, 569–580 (2018). doi: 10.1007/s11663-018-1187-x
17. H. Yu, X. Liu, H. Bi, Deformation behavior of inclusions in stainless steel strips during multi-pass cold rolling, J. Mater. Process. Technol. **209**, 4274–4280 (2009)
18. Y. Zeng, H. Fan, X. Xie, Effects of the shape and size of rectangular inclusions on the fatigue cracking behavior of ultra-high strength steels, Int. J. Miner. Metall. Mater. **20**, 360–364 (2013). doi: 10.1007/s12613-013-0735-2

Cite this article as: Julie Godon, Pascal Antoine, Jean Bernard Vogt, Jérémie Bouquerel, Influence of steel cleanliness on drawability of fine filaments with high tensile strength, Metall. Res. Technol. **116**, 513 (2019)